Dalton Transactions

Accepted Manuscript

1

Vibrational spectroscopic studies and DFT calculations on NaCH₃CO₂(aq) and CH₃COOH(aq).

Wolfram W. Rudolph[1]* Dieter Fischer[2] and Gert Irmer[3]

1) Medizinische Fakultät der TU Dresden, Institut für Virologie im MTZ, Fiedlerstr. 42
   01307 Dresden, Germany; e-mail: Wolfram.Rudolph@tu-dresden.de.
* corresponding author

2) Institute of Polymer Research Dresden, Hohe Straße 6, 01069 Dresden, Germany.

3) Technische Universität Bergakademie Freiberg, Institut für Theoretische Physik,
   Leipziger Str. 23, 09596 Freiberg, Germany

18.11.2013　　　revised manuscript　　17:15

2

Abstract

Aqueous solutions of sodium acetate, $NaCH_3CO_2$ and acetic acid, CH_3COOH were studied using Raman and infrared spectroscopy. The spectra were recorded over a large concentration range, in the terahertz region and up to 4000 cm^{-1}. In the isotropic Raman spectrum in R-format, a polarized band at 189 cm^{-1}, was assigned to the ν_1 Na-O stretch of the hydrated Na^+- ion and a shoulder at 245 cm^{-1} to the restricted translation band, ν_s O-H···O* of the hydrated acetate ion, $CH_3CO_2^-(aq)$. The $CH_3CO_2^-(aq)$, and the hydrated acetic acid, $CH_3COOH(aq)$ possess pseudo C_s symmetry. Geometrical parameters for the species in the gas phase and for $CH_3CO_2^-(aq)$ and $CH_3COOH(aq)$ are reported. Characteristic bands for $CH_3CO_2^-(aq)$ and $CH_3COOH(aq)$ were assigned under the guidance of the DFT vibrational frequency calculations and discussed in detail. In aqueous $NaCH_3CO_2$ solutions, at high concentrations, no contact ion pairs could be detected but instead solvent separated ion pairs were found. In $LiCH_3CO_2(aq)$, however, contact ion pairs are formed which is indicated by the appearance of a shoulder at 939 cm^{-1} and the shift of the symmetric stretching mode of the $-CO_2^-$ group to higher wavenumbers.

3

1. Introduction

Recent interest in studying carboxylates and carboxylic acids in aqueous solution stems from their importance as constituents in biomolecules such as amino acids, fatty acids and surfactants among others [1-3]. Detailed studies aimed at the hydration, dissociation and ion-pair formation of these species in solution were carried out by infrared [3-5] and dielectric relaxation spectroscopy (DRS) [6,7]. DRS studies are useful in determining hydration numbers and association constants in electrolyte solutions forming ion pairs such as solvent shared-, solvent-solvent separated ion pairs and ion pairs without interposed water (contact ion pairs, CIPs). Such studies were carried out on aqueous solutions of sodium salts of acetate ($CH_3CO_2^{-\,1}$), and formate (HCO_2^-) as well as trifluoroacetate ($CF_3CO_2^-$) [6,7]. Hess and Vegt [1] studied the interaction of alkali metal cations with carboxylate ions in aqueous solution, in an effort to unravel cation specific binding with protein surface charges. They concluded the existence of solvent separated ion pairs in aqueous solution between the monovalent cations and acetate according to the following order: $K^+ < Na^+ < Li^+$. Additionally, selective binding of alkali metal ions with carboxylate by x-ray absorption spectroscopy were studied [2] supporting the Law of Matching Water Affinities [8] invoking ion pairing to explain Hofmeister effects on proteins.

Although the sodium salts of acetate were measured in solid state by infrared and Raman spectroscopy [9-13], only a few solution spectra were reported in the literature [11,14]. No systematic studies were carried out in aqueous solution or solutions of heavy water. However, over the years acetate solutions of divalent metal ions were reported for zinc(II)-, lead(II)-, nickel(II)-, copper(II)-, magnesium(II) and calcium(II) [14-18].

In this study, Raman and infrared spectra of $NaCH_3CO_2$ were measured in solution of water and heavy water over a very broad concentration range. Raman spectra were measured to low Raman frequencies at ~45 cm^{-1}, the terahertz spectral region, which is of recent interest in studying electrolyte solutions [19]. In very dilute solutions, the acetate ion should be completely hydrated and such a species may serve as a reference for the ligated acetate in acetato complexes. On the other hand, hydration of the Na^+ cation in aqueous solution, probably a flexible -coordinate sphere [20-25], plays a role in characterizing these aqueous solutions. Such metal ion-water bands were already characterized for a variety of mono-, and divalent cations [26-31,33,34]. Therefore, Raman spectroscopic measurements at the low frequency region were carried out to extract the isotropic scattering component of the Na-O stretching mode of the aqua-sodium(I) species. This low

---

[1] The formula of the acetate ion was written as $CH_3CO_2^-$ throughout the text in order to elucidate the resonance hybrid form of the carboxylate group (delocalized electron). Sometimes it is also written as CH_3COO^-.

4

frequency region should also allow the characterization of the restricted translational band, ν_s O-H$\cdots$O*, between H_2O and $CH_3CO_2^-$.

The DFT frequency calculations of the normal modes were carried out to assist in assigning the spectrum of the hydrated acetate ion, $CH_3CO_2^-$(aq). In addition, geometrical parameters such as bond length and bond angles were obtained by DFT calculations. The DFT parameters were reported in both the gas phase and the hydrated form by applying a continuum solvation sphere.

Finally, dilute solutions of acetic acid were measured and the vibrational modes assigned. DFT calculations were carried out for CH_3COOH to assist the assignments of the vibrational bands and report on the geometrical parameters in the gas phase and with a solvation sphere.

2. Experimental Section

<u>Preparation of the solutions:</u> A $NaCH_3CO_2$ stock solution was prepared by weight from dried anhydrous $NaCH_3CO_2$ (99.5 % ReagentPlus, Sigma-Aldrich) with triply distilled water free of CO_2. The solution densities were determined with a pycnometer of 5.000 mL volume at 23 ± 0.1 °C. From the solution densities and the concentrations in $mol\cdot L^{-1}$, the concentrations in $mol\cdot kg^{-1}$ were calculated and from the latter, the R_w – values were determined. R_w – values represent the number of moles of water per one mole of salt. The stock solution was 5.022 $mol\cdot L^{-1}$ ($R_w = 8.54$). Further, $NaCH_3CO_2$ solutions were prepared: 2.184 $mol\cdot L^{-1}$ ($R_w = 22.90$), 1.209 $mol\cdot L^{-1}$ ($R_w = 43.40$), 0.810 $mol\cdot L^{-1}$ ($R_w = 65.97$), 0.161 $mol\cdot L^{-1}$ ($R_w = 343.21$), and 0.0325 $mol\cdot L^{-1}$ ($R_w = 1704.8$). The sodium acetate solutions react alkaline. The pH value of a 0.161 $mol\cdot L^{-1}$ solution was measured at 8.40 (23 °C). The acetate solutions were sealed in air tight plastic bottles to prevent the uptake of CO_2 from air.

Three $NaCH_3CO_2$ solutions in heavy water were prepared by weight from dried anhydrous $NaCH_3CO_2$ and heavy water (99.9 % D; Merck, Darmstadt, Germany) with concentrations of 3.944, 0.789 and 0.262 $mol\cdot L^{-1}$.

Lithium acetate solutions were prepared from $LiCH_3CO_2\cdot 2H_2O$ (Sigma-Aldrich, reagent grade) using triply distilled water by weight.

The CH_3COOH solutions were prepared by weight from glacial acetic acid (Merck, Darmstadt, pro Analysi) and triply distilled water.

<u>Raman spectra:</u> Raman spectra were measured in the macro chamber of the T 64000 Raman spectrometer from Jobin Yvon in a 90° scattering geometry at (23 ± 0.4) °C. The solutions were measured in high precision quartz cuvettes from Hellma Analytics (Müllheim, Germany) which were sealed with an air tight stopper. The spectra were excited with the 487.98 nm line of an Ar^+ laser at a power level of ~ 1100 mW at the sample. After passing the spectrometer in subtractive mode, with gratings of 1800 grooves/mm, the scattered light was detected with a cooled CCD

detector [32]. I_{VV} and I_{VH} spectra were obtained with fixed polarisation of the laser beam by rotating the polarisator at 90 ° between the sample and the entrance slit to give the scattering geometries: I_{VV} = I(Y[ZZ]X) = $45\alpha'^2 + 4\gamma'^2$ and I_{VH} = I(Y[ZY]X) = $3\gamma'^2$. The isotropic spectrum, I_{iso} is then constructed: $I_{iso} = I_{VV} - 4/3 \cdot I_{VH}$ [32]. The depolarization ratio, ρ, of the modes was determined according to: $\rho = I_{VH}/ I_{VV} = 3\gamma'^2/(45\alpha'^2 + 4\gamma'^2)$ and the procedure of measuring the depolarization ratios described in detail in ref. [32].

The wavenumber positions were checked with Neon lines and the peak positions for bands with smaller band width (full width at half height; fwhh) were determined with an error of ± 0.25 cm^{-1} and broader bands fwhh ≥ 25-30 cm^{-1}) with a precision of ± 1 cm^{-1}. The signal to noise ratio for the band at 928 cm^{-1} of the spectra for a 0.810 mol$\cdot$L^{-1} solution was determined to 420 : 1 and was much better for species in more concentrated solutions.

Band intensities were determined by fitting the bands using Gaussian-Lorentzian product functions on baseline corrected spectra. Band intensities for $CH_3CO_2^-$(aq), and $CH_3CO_2^-$(D_2O) were presented so that the strongest mode was set to 100.00 and the band intensities of the other modes relative to this value. The details of the band fitting procedure of the baseline corrected Raman- and infrared- bands were described elsewhere [34]. Spectra in R-format were obtained and are of necessity in the low frequency range. Further details were published elsewhere [32].

<u>Infrared spectra:</u> The FT-IR spectrometer Equinox 55 (BRUKER OPTICS, Germany) [33] was used in the wavenumber range from 400 to 4000 cm^{-1} with a spectral resolution of 2 cm^{-1} in capillary thickness between AgCl disks. Sixty four scans were obtained. The spectra were corrected by subtracting the spectra of the window (AgCl) material from the measured solution spectra. A series of aqueous $NaCH_3CO_2$ solutions (2.184 1.209, 0.810, and 0.161 mol$\cdot$L^{-1}) were measured. In order to quantify the infrared bands, the water spectrum, measured under the same conditions, was subtracted from the spectra of the $CH_3CO_2^-$(aq).

<u>Density Functional Theory calculations:</u> The optimization of the molecular geometry and the calculation of the vibrational frequencies were performed with the Density Functional Theory (DFT) method B3LYP using the basis set 6-311++(3df,2pd) and employing the program suite Gaussian 03 [35]. Proper description of anions with electrons which are located, on average, relatively far from the nuclei, require diffuse orbitals and polarization basis sets. The optimization procedure resulted in a geometry of the $CH_3CO_2^-$ with the dihedral angle $\varphi = 0°$ as a stable configuration and no imaginary frequencies were obtained. Furthermore, DFT frequency calculations were performed for this stable configuration in the gas phase. A second geometry at the dihedral angle for $\varphi \sim 29°$ corresponds to a saddle point on the potential energy surface (PES). In order to ensure adequate convergence and

reliability of the computed frequencies, very tight optimization convergence criteria and ultrafine integration grids were used.

In addition to the calculations of the anion in the gas phase, calculations were also performed in the presence of the solvent water by placing the solute within the solvent. The latter was modelled as an isotropic and homogeneous continuum, characterized by its dielectric properties. The frequencies were calculated with a floating cavity (a set of interlocking spheres attached to the solute atoms). The electrostatic solute-solution interaction was calculated introducing an apparent charge distribution spread on the cavity surface. The Polarized Continuum Model (PCM) implemented in the GAUSSIAN package was used in a version described in ref. [36]. The orientational component of the solvent polarization is not able to follow the oscillating charge distribution connected with fast vibrations. Only the faster contributions to the solvation polarization are instantaneously equilibrated to the momentary charge distribution. In studies of non-equilibrium effects within the PCM it was found that non-equilibrium solvation has greater effects on the calculated Raman and IR intensities but little effect on the frequencies [37,38].

A similar optimization procedure was carried out for CH_3COOH. The DFT frequencies were calculated for the stable geometry with C_s symmetry in the gas phase and with a complete solvation sphere.

3. Results and discussion

The present study has been organized in the following manner: first, results are presented on the terahertz region of aqueous $NaCH_3CO_2$ solutions characterizing the Na-O stretching mode of the hydrated Na^+ ion and the restricted translation band of the O-H···O* unit formed between $CH_3CO_2^-$ and water. Next, $CH_3CO_2^-(aq)$ bands are characterized and assigned vibrational modes with the help of the theoretical frequencies derived from the DFT calculations. Furthermore, ion pairs which may form in aqueous $NaCH_3CO_2$ solution are characterized and discussed and, finally dilute hydrated acetic acid solutions are studied and band assignments completed guided by DFT calculated frequencies.

3.1. Characterization of terahertz frequency region

Aqueous solutions of $NaCH_3CO_2$ are quite strongly dissociated forming $Na^+(aq)$ and $CH_3CO_2^-$ (aq) ions. However, at higher concentrations, ion pair formation must be taken into account. In concentrated $NaCH_3CO_2$ solutions, the ion pairs formed are most probably with water molecules interposed between Na^+ and $CH_3CO_2^-$. DRS investigations of sodium acetate (and trifluoroacetate) solutions revealed, after the correction of earlier results [6], that no direct contact between Na^+ and these ions could be detected [7] and the results reinforced by Hess and Vegt [1]. The types of ion pairs will change significantly with dilution, namely, from outer-sphere ion pairs to outer-outer-

sphere ion pairs and finally completely hydrated ions formed in very dilute solutions (≤ 0.001 molL^{-1}). Inspection of our Raman spectral data as a function of solute concentration and taking into account the published DRS data on $NaCH_3CO_2$, it is possible to characterize the ion pairs formed. Furthermore, the Na^+ ion in aqueous solution is hydrated and most of the recent simulations, XRD and neutron diffraction studies, revealed that the Na^+ ion is hydrated by ~5 water molecules in the first sphere, although the hydration sphere is quite flexible [20-25]. The residence time of a water molecule in the first hydration sheath of $[Na(OH_2)_5]^+$ is extremely short, i.e. shorter than the residence time of $[Li(OH_2)_4]^+$ at ~ 1 ns [39,40]. In contrast to Na^+, the Li^+ ion forms a tetrahydrate in aqueous solution [26-28,39,40]. The terahertz isotropic Raman spectrum revealed the nature of the first hydration sphere of $Li^+(aq)$ and a well-defined isotropic mode, ν_1 LiO_4, was detected at 255 cm^{-1} in solutions of LiCl, LiBr and $LiClO_4$ [28]. An inspection of the isotropic Raman spectra in $NaCH_3CO_2$ solutions and neat water at low frequencies between $45 - 500$ cm^{-1} leads to the conclusion that a broad band at 189 cm^{-1} in the terahertz frequency region (Figure 1B) is due to the ν_1 Na-O stretch of $[Na(OH_2)_5]^+(aq)$. The band is very broad though and reflects the possibility that the first hydration sphere is ill defined. A neutron scattering study combined with Raman spectroscopic measurements revealed an isotropic band at 185 cm^{-1} quite close to our value [20]. Most of the values for the first hydration number were given at ~5 [22-24] and an internuclear bond distance of Na-O at 2.34 Å [22]. The influence of water in the first hydration sphere of Na^+ on the water deformation band at 1641 cm^{-1}, and the very broad stretching band (double band at 3235 and 3400 cm^{-1} and shoulder at 3635 cm^{-1}) is difficult to ascertain because the influence of the hydrated anion is not easy to separate from those of $[Na(OH_2)_5]^+$.

In addition to the Na-O stretching mode at 189 cm^{-1}, a broad band contribution at 245 cm^{-1} appeared (Figure 1B) and was assigned to the restricted translation band, ν_s O-H$\cdots$O, reflecting the strong H-bonds between both oxygen atoms of the $-CO_2^-$ group and H_2O [41]. This restricted translational mode, determined by acetate water hydrogen bonds, becomes less important with dilution and in dilute acetate solutions this mode appears as a weak polarized band at 175 cm^{-1} due to O$\cdots$H-O bonds between water molecules.

3.2. Characterization of $CH_3CO_2^-(aq)$ in $NaCH_3CO_2(aq)$

The polyatomic anion $CH_3CO_2^-$, though investigated in the solid state as $NaCH_3CO_2(cr)$ was not studied in any systematic way in aqueous solutions. Acetato-complexes of divalent cations, on the other hand, were characterized in solution more frequently [14-18]. For completeness, an overview Raman spectrum of $NaCH_3CO_2(cr)$ is given in Figure S1, Suppl. Material. Subtle changes of the solution spectrum of $CH_3CO_2^-(aq)$ occur compared with the spectrum of $NaCH_3CO_2(cr)$ and indeed were detected. In order to shed light on the nature of $CH_3CO_2^-(aq)$, the acetate spectrum in solution

was followed from very high concentrations to very dilute solutions. Extrapolation to zero concentration, the band parameters of the characteristic modes of the $-CO_2$ group, which is where the coordination to the cation takes place, gives the parameters for infinitely dilute solution free of the cation influence. $CH_3CO_2^-$ spectra in D_2O were measured in order to characterize the antisymmetric stretching mode of the CO_2 group undisturbed from the deformation mode of water at 1641 cm^{-1}.

3.2.1. DFT calculations: geometrical parameters and symmetry of $CH_3CO_2^-$

A*b initio* cluster calculations of the type $CH_3CO_2^- \cdot H_2O_n \cdot H_2O_m$ (n = first sphere water molecules, and m = second sphere molecules) [41] revealed that both oxygen atoms of the $-CO_2^-$ group are hydrated with up to 6 water molecules in the first sphere where the waters form single H-bonds with the oxygen atoms. The seventh water molecule is located in the second sphere. This fact is relevant for the symmetry of the acetate ion in aqueous solution (water cage). Unfortunately, no frequency calculations on these acetate water clusters were completed. Recent QM/MM dynamics simulations [42], combined X-ray diffraction and NMR studies [43] and neutron diffraction measurements [44] reinforced this *ab inition* model and revealed that $CH_3CO_2^-$ is surrounded by up to 6 water molecules which fluctuate forming loosely and tightly bound water molecules of the type C-O···HOH [42]. The hydration sphere around the $-CO_2^-$ group is quite flexible. The assumed symmetry C_{2v} for $CH_3CO_2^-$ stated earlier in the literature is not correct, however (9-11,15-17,49). This model should be rejected because it does not explain the large number of observed polarized modes in solution.[2] The isotropic scattering contribution at 245 cm^{-1}, mentioned previously, represents the broad restricted translation mode of the O-H···O* bonds formed between the oxygen atoms of $CH_3CO_2^-$ and water molecules. This flexible hydration structure of $CH_3CO_2^-$(aq) also leads to a slightly asymmetric environment and therefore the symmetry is, strictly speaking, C_1 (pseudo C_S with small deviations). (One possible form of the H-bonding may be bifurcated H-bonds. However, the hydration of both oxygen atoms of the acetate ion with up to 6 water molecules was shown to be a realistic picture of the hydration in solution [41-44].)

The DFT calculations in the gas phase generated a stationary point on the PES with a local minimum for the $CH_3CO_2^-$ ion possessing C_S symmetry. The most stable C_s geometry of $CH_3CO_2^-$ anion is a one with a dihedral angle $\varphi = 0°$ (structure $C_s(\mathbf{I})$) as shown in Figure 2. The geometrical parameters such as bond lengths and bond angles are presented in Table 1 for the anion *in vacuo* and for the ion with a solvation (i.e. hydration) sphere. The DFT parameters of both acetate structures (see Table 1) show subtle differences especially the shorter C-C bond distance and the longer C-O bond distances of the hydrated form compared with the one *in vacuo*. For the $C_s(\mathbf{I})$ conformer, five

---

[2] In earlier publications the acetate ion was reported having C_{2v} symmetry and for the irreducible representation it would follow: Γ_{vib} (C_{2v}) = $5a_1 + a_2 + 5b_1 + 4b_2$. But this symmetry resulted from the earlier days of G – F matrix method calculations and was intended to simplify the calculations at a time when computational power was limited [48].

atoms lie on the mirror plane, namely H5-C1-C2-O3-O4. The mirror plane dissects the molecule (Figure 2) in such a way that the two oxygen atoms of the -CO_2 group are no longer equivalent and which is why both of the stretching modes of the -CO_2 group are polarized, namely $\nu_s CO_2$ quite strongly and the other, $\nu_{as}CO_2$, is weakly polarized in the Raman effect. The deformation mode of the CO_2 group, $\delta\, CO_2$, appears polarized.

A second C_s structure with the dihedral angle $\varphi = 29°$ for $CH_3CO_2^-$ is a saddle point at the PES (structure **II,** Figure S2 and Table S2, Suppl. Material). In this case, four atoms lie in the mirror plane, namely C1-C2-O3-O4 and both oxygen atoms are equivalent which is why the two stretching modes of the -CO_2 group $\nu_s CO_2$ and $\nu_{as}CO_2$ are polarized and depolarized, respectively.

The geometry for $\varphi = 0°$ for structure **I** is 11 cal/mol lower in energy than the structure **II**. These two conformers have very low frequency torsional modes. The potential energy distribution of the gas phase structure, depending on the dihedral angle φ, is presented in Figure S3, Supplementary Material. Because of the small energy difference compared with the thermal energy quantum kT (576 cm^{-1} at 290 K) between these two conformers, at room temperature, the rotation of the C-C bond may be nearly free in the gas phase.

However, in aqueous solution, the free rotation of the acetate may be strongly hindered because it interacts with the water molecules in a "cage like" structure. Both oxygen atoms form strong H-bonds while the -CH_3 group interacts weakly [42].[3]

3.2.2. Normal modes of $CH_3CO_2^-$(aq)

The Raman and infrared spectroscopic data for dilute $NaCH_3CO_2$(aq) are summarized in Table 2 and an overview Raman spectrum of a 5.022 molL^{-1} presented in Figure 3A, while an infrared spectrum is shown in Figure 3 B. Raman- and infrared- spectroscopic concentration plots of four $NaCH_3CO_2$ solutions are presented in Figures 4 and 5, respectively.

The 15 normal modes of $CH_3CO_2^-$ of structure **I** (Figure 2) belong to the point group C_s and span the representation: Γ_{vib} (C_s(**I**)) = 10 a$'$ (Ra, i.r.) + 5 a$''$ (Ra, i.r.). All modes are Raman and i.r. active and those with the character a$'$ are partially polarized while the ones with symmetry a$''$ are depolarized. The 15 normal modes of $CH_3CO_2^-$ of structure **II** span the irreducible representation: $\Gamma_{vib}(C_s$(**II**)) = 9 a$'$ (Ra, i.r.) + 6 a$''$ (Ra, i.r.). This conformer has one polarized Raman band less than structure **I** (10 polarized modes for structure **I** but 9 for structure **II**). The DFT frequencies for structures **I** and **II** are quite similar and with the broad bands in aqueous solution such small differences are of little consequence.

Inspection of the spectra in Figures 3 -5 and the data in Table 2 leads to the conclusion that

---

[3] Free rotation around the C-C bond of acetate was observed and investigated using electron spin resonance in crystals of $CH_3CO_2Na*D_2O$ [45] and in crystals of lithium acetate dihydrate using neutron diffraction [46]. Spectral evidence for the rotation of the methyl group in liquid toluene was given in [47].

10

two distinct vibrational regions may be discussed: A) a region from 400-1700 cm^{-1} and B) from 2800- 3100 cm^{-1}. The vibrational modes are mixed on the PES and therefore the assignment of the normal modes is difficult. However, the DFT calculations were an excellent guide in assigning the fundamental modes of $CH_3CO_2^-$(aq) (structure **I** + solvation sphere**)**. The form of the normal modes for the hydrated anion is illustrated in Figure 6.

Region A: The normal mode with the lowest calculated frequency 22.9 cm^{-1} is a pure torsional motion along the C-C bond and could not be observed experimentally. Three bands are expected in the region from 400-700 cm^{-1} whose origin can reasonably be attributed to the rocking and deformation modes of the -CO_2 group. The mode at 474 cm^{-1} (DFT result at 447.1 cm^{-1}) represents a rocking mode of the -CO_2 group which couples quite severely with the out-of-plane deformation of the -CH_3 group. The Raman mode at 620.7 cm^{-1}, also depolarized, with the theoretical value at 624.3 cm^{-1} was assigned to a rocking mode of the -CO_2 group. The polarized deformation mode was assigned to a mode at 654.2 (DFT value at 632.7 cm^{-1}). These modes at low frequencies are shown in Figures 1A and 3A and B. The strongly polarized Raman mode at 928.3 cm^{-1} (fwhh = 12.35 cm^{-1}) was assigned to the C-C stretch. The mode mixes strongly with δ OCO. The C-C stretching mode of $CH_3CO_2^-$(aq) showed a small but distinct concentration dependence in such a way that the peak position shifted to higher wavenumbers and the band width increased. In a dilute $NaCH_3CO_2$(aq) the ν C-C mode appears at 928.3 cm^{-1} and showed a band width at 12.35 cm^{-1}.

The modes at 1021.5 and 1052 cm^{-1} were assigned to rocking modes of the CH_3 group and the mode at 1347.6 cm^{-1} was assigned to a deformation mode of the CH_3 group. The Raman band at 1413.5 cm^{-1} is polarized at ρ = 0.26 and was assigned to the stretching mode of the -CO_2 unit, $ν_sCO_2$. The $ν_sCO_2$ mode broadens with concentration and the fwhh as a function of solute concentration is presented in Figure S4. This mode is strong in both the Raman effect and infrared. The bands at 1426 and 1440 cm^{-1} were assigned to deformation modes of the CH_3 group. These weak, broad bands are completely overlapped by the strong mode at 1413.5 cm^{-1}. The weak Raman band at 1556 cm^{-1} is, however, the strongest infrared mode and was assigned to the asymmetric stretch of the -CO_2 group. The advantage of measuring $CH_3CO_2^-$ in D_2O is that in solution of heavy water the antisymmetric stretch, $ν_{as}CO_2$, can be obtained undisturbed from the broad deformation band of water at 1641 cm^{-1}. This is especially relevant in dilute solutions. The measured Raman bands and their assignments of $CH_3CO_2^-$(D_2O) are given in Table S1. However, the stretching bands, $ν_sCO_2$ and $ν_{as}CO_2$ of $CH_3CO_2^-$(D_2O) appeared slightly shifted at 1417.8 cm^{-1} (fwhh = 22 cm^{-1}) and 1563 cm^{-1} (fwhh = 42 cm^{-1}). Slight shifts also occur for the other modes (Table S1). This is due to the change of intramolecular coupling of the acetate modes with a

change of H to D of the solvent. Although the naked acetate ion contains neither H nor D, the fact that the anion is strongly hydrated (deuterated) causes this coupling of the intramolecular modes.

The comparison of the two calculated stretching modes of $CH_3CO_2^-$ *in vacuo* for ν_sCO_2 at 1350.8 cm^{-1} and for $\nu_{as}CO_2$ at 1650.4 cm^{-1} with the species in solution, $CH_3CO_2^-(aq)$ resulted in experimental wavenumbers for both modes at 1413.5cm^{-1} and at 1556 cm^{-1} (data in Table 2). These large shifts for the stretching modes ν_sCO_2 and $\nu_{as}CO_2$ of +62.7 cm^{-1} and -94.4 cm^{-1} considering the $CH_3CO_2^-$ *in vacuo* and the hydrated form, $CH_3CO_2^-(aq)$ reflects the strong hydration effect of the $-CO_2$ group in aqueous solution.

The vibrational modes of the $-CO_2$ group are characteristic for all salts of carboxylic acids [3,14,51-53]. In the tribromoacetate spectrum e.g., $CBr_3CO_2^-(aq)$ [53] the bands of the symmetric stretch of the $-CO_2$ group appeared at 1332 cm^{-1} as a polarized band ($\rho = 0.18$) and the antisymmetric stretch at 1651 cm^{-1} was slightly polarized ($\rho = 0.69$). The antisymmetric stretching mode of the $-CO_2$ group is the strongest band in the infrared spectrum and is used as a diagnostic band.

Region B: The band at 2935.5 cm^{-1}, the strongest mode in Raman, and much weaker bands at 2984 and 3014 cm^{-1} were assigned to the stretching bands of the CH_3 group. It is well known that the ν C-H modes are in Fermi resonance with the deformation modes of the CH_3 group [50] at 1440 cm^{-1} and therefore ν_s C-H at 2935.5 cm^{-1} appeared energy distorted. On the other hand, the uncoupled mode of C-H occurs at 2971 cm^{-1} for $CHD_2CO_2^-(aq)$ leading to the undisturbed mode at 2943 cm^{-1}.

For completeness of the spectroscopic assignments, weaker bands observed in the Raman and infrared spectrum were attributed to combination and overtone bands and are presented in Table 3 together with the tentative assignments.

3.2.3. Ion pair formation of Na^+ with $CH_3CO_2^-$

In the 5.022 mol·L^{-1} NaCH$_3$CO$_2$(aq) the C-C stretching mode located at 928.8 cm^{-1}, has shifted by 0.5 cm^{-1} to higher wavenumbers compared to its extrapolated value at zero concentration. The half width of the same band possesses a fwhh at 13.3 cm^{-1} compared to its extrapolated value at zero concentration at 12.35 cm^{-1}. A concentration profile of baseline corrected isotropic Raman spectra of the ν C-C mode is given in Figure 7A and the graph of the concentration dependence of the peak position and the fwhh for this mode is given in Figure 7B. The symmetric band profile remains the same over the solute concentration. The symmetric stretching mode, ν_s CO$_2$ has shifted slightly to higher wavenumbers with increasing solute concentration and the half width increased as well. In the 5.022 mol·L^{-1} NaCH$_3$CO$_2$(aq), ν_s CO$_2$ appeared at 1415 cm^{-1} and possessed a fwhh at ~28 cm^{-1} whereas the peak position and fwhh extrapolated to zero concentration were 1413.5 cm^{-1} and 24 cm^{-1}, respectively. It becomes clear that in such a concentrated solution with a solute : water ratio of 1: 8.54, the ion pairs of the outer-sphere type have to be invoked. On the one hand, in this concentrated

12

solution there is simply not enough water to form a complete second hydration sphere which would warrant an outer-outer sphere ion pair type (ion pairs with two interposed waters) while on the other hand, no signs for CIPs were observed. Solvent separated ion pairs formed may be formulated as $[Na^+(OH_2)CH_3CO_2^-]$ in concentrated $NaCH_3CO_2(aq)$. A direct contact of $CH_3CO_2^-$ via one or two oxygen atoms with Na^+ must lead to a change of both the electronic structure of the ligated acetate and the force field which would lead in turn to a more pronounced change of its vibrational spectrum. This, however, was not observed.

In order to further study the complex formation in $NaCH_3CO_2(aq)$ a ternary solution of $NaCH_3CO_2$ plus an additional amount of NaCl was analyzed. Probing a 0.689 $molL^{-1}$ $NaCH_3CO_2$ solution with an additional 4.257 $mol \cdot L^{-1}$ NaCl (common-ion effect) would cause a shift of the equilibrium towards the CIPs, if they exist. However, no spectroscopic signs of CIP formation were observed. On the contrary, the isotropic ν C-C mode was narrow (fwhh = 12.1 cm^{-1}) and showed no shoulder or a separate mode and thus no indication of contact ion pair formation. The $\nu_s CO_2$ mode also showed no signs of CIP formation indicated by its peak position and fwhh which did not change compared with the band parameters for dilute $NaCH_3CO_2(aq)$. In the terahertz region of the Raman spectrum, a comparison of a NaCl(aq) with the ternary solution of $NaCH_3CO_2$ plus additional NaCl, did not reveal any sign of contact ion pair formation either. From these spectroscopic observations, only one conclusion could be drawn, namely, that no CIPs exist in $NaCH_3CO_2(aq)$.

In $LiCH_3CO_2(aq)$, however, CIPs were formed which was indicated by a band component of the ν C-C mode at 939 cm^{-1} and the shift of $\nu_s CO_2$ to higher wavenumbers. In a ternary solution of a 0.930 $molL^{-1}$ $LiCH_3CO_2$ plus additional LiCl (13.23 $mol \cdot L^{-1}$), the ligated acetate with Li^+ dominated the spectrum completely (see Figure 8). The formation of the ion pairs may be formulated according to eq. (1): $[Li(OH_2)_4]^+ + CH_3CO_2^- \leftrightarrow [(H_2O)_2LiO_2CH_3]^0 + 2H_2O$ (1)
assuming a bidentate acetato complex with Li^+.

3.3 . Solution spectra of $CH_3COOH(aq)$

The geometry of CH_3COOH monomer in the gas phase is stable at a dihedral angle $\varphi = 0°$ and possesses C_S symmetry (Figure 9). This structure, the *trans* conformer, which corresponds to a stationary point on the PES is a local minimum which results in real frequencies for all modes. The *cis* conformer, however, is less stable. A detailed *ab initio* study on CH_3COOH conformers in the gas phase was carried out recently [54]. The geometrical parameters of CH_3COOH in the gas phase and with a complete solvation sphere is presented in Table S3. The DFT frequencies were compared with the data measured by Raman and infrared spectroscopy and the data summarized in Table 4. In concentrated aqueous solutions of carboxylic acids with a mole ratio acid : H_2O < 1 to 4-5, the carboxylic acids are no longer in their hydrogen bonded linear structure but are hydrated [14].

Subsequent hydration takes place and increases with further dilution. The 18 vibrational modes of CH$_3$COOH correspond to symmetry C$_s$ and span the representation: Γ_{vib} (C$_s$) = 12 a$'$ (Ra, i.r.) + 6 a$''$ (Ra, i.r.). All modes are Raman and i.r. active and the modes with the character a$'$ are partially polarized while the ones with symmetry a$''$ are depolarized.

The acetic acid solutions at higher concentrations contain linear and cyclic associates but increasing dilution leads to the formation of the hydrated acid in its monomeric form. The Raman spectra of a 0.121 mol·L^{-1} solution with the polarized, depolarized and isotropic scattering are presented in Figure 10.

In dilute solutions, the acetic acid is completely hydrated ($< \sim 0.1$ molL^{-1}) and further dilution should lead to the formation of the dissociation product, CH$_3$CO$_2^-$(aq). However, even in quite dilute solutions only small amounts of the conjugate base, CH$_3$CO$_2^-$(aq) are formed because acetic acid is weak (pK$_a$ = 4.757; 25 °C [55]). The dissociation scheme may be defined according to eq. 2:

$$CH_3COOH \ + \ H_2O \ \leftrightarrow \ CH_3CO_2^- \ + \ H_3O^+ \tag{2}.$$

The most prominent band of the acid, the mode at 1713 cm^{-1} (Figure 11, right panel) was assigned to ν C=O of the COOH group, which may be used for analytical purposes. It is noteworthy that the modes of the CH$_3$ group are similar to ones of the acetate ion and because of their rather large half width they could not be easily distinguished from the ones in CH$_3$CO$_2^-$(aq) (results in Table 2 and 4). In Figure 11, left panel, the ν C-C mode of the isotropic Raman profile (water spectrum subtracted) is presented for a dilute aqueous CH$_3$COOH solution at 0.0246 mol·L^{-1} (R$_w$ = 2241.4). The ν C-C mode of CH$_3$COOH(aq) at 893 cm^{-1} (fwhh = 19 cm^{-1}) was assigned to the acetic acid but at higher frequencies the very small band at 928.4 cm^{-1} assigned to ν C-C of CH$_3$CO$_2^-$(aq). The isotropic Raman profile (water spectrum subtracted), of ν C=O band of the same aqueous CH$_3$COOH solution is shown in Figure 11, right panel. The ν C=O mode appeared at (1713 ± 1) cm^{-1} with a fwhh at (39.5 ± 2) cm^{-1}.

The graphical description for the normal modes is given in Figure 12. Again, the modes couple quite strongly. The 6 normal modes which lose their symmetry during vibration (depolarized) with respect to the mirror plane (a$''$) reduce to C$_1$ symmetry and the projection of the strong displacement vectors are shown perpendicular to the mirror plane. Displacements also occur due to the invariance of the mass centre in the mirror plane but these projections are not shown. For the 12 modes with symmetry a$'$, the polarized modes, the symmetry of the species during vibration remains.

To summarize, the most prominent band of the acid is the mode at 1713 cm^{-1} assigned to ν C=O of the -COOH group. The depolarization degree, ρ, for the C=O stretch at ~0.1 is small but typical for all carboxylic acids (refs. [51,52]). The ν C-C stretch of CH$_3$COOH(aq) appeared at 893 cm^{-1} and with sufficient dilution the ν C-C stretch of its corresponding base, CH$_3$CO$_2^-$(aq) was detectable. The

C=O stretching mode, ν C=O, was followed to very dilute solutions and its band parameters were measured. The stretching mode of the C-(OH), ν C-O appeared at ~1365 cm^{-1} overlapped with δ CH$_3$ at ~1380 cm^{-1} as a weak band in Raman but quite strong in infrared absorption. The deformation mode of the -COOH group appeared at 600 cm^{-1} in Raman but was completely overlapped by the very strong and broad rocking mode of water in infrared. The stretching mode of O-H, ν OH, although prominent too, is, in dilute solution, broad and completely overlapped with the broad and strong OH contour of water. The deformation mode, δ C-O-H appeared at ~1290 cm^{-1} in both the Raman effect and infrared absorption.

4. Conclusions

Solutions of NaCH$_3$CO$_2$ and its corresponding acid, CH$_3$COOH, were studied by Raman and infrared spectroscopy as a function of solute concentration. In the isotropic Raman spectra in R-format at the terahertz frequency range, an isotropic mode at 189 cm^{-1} was observed as the one belonging to the ν$_1$ stretching mode of [Na(OH$_2$)$_5$]$^+$(aq). The restricted translation mode, ν$_s$ O-H⋯O* of the hydrated CH$_3$CO$_2^-$ appeared at 245 cm^{-1} in the isotropic R-scattering. Furthermore, in the NaCH$_3$CO$_2$ solution spectra, CH$_3$CO$_2^-$(aq) was assigned according to symmetry C$_s$. Characteristic bands of CH$_3$CO$_2^-$(aq) are discussed and particular attention is paid to bands of the –CO$_2^-$ group such as the rocking mode at 474 cm^{-1}, the deformation mode at 654 cm^{-1} and the symmetric and anti-symmetric stretching mode at 1414 cm^{-1} and 1556 cm^{-1}. The characteristic band of CH$_3$COOH(aq) is the polarized band at 1713 cm^{-1}. For CH$_3$COOH(aq) the stretching mode, ν C-C, at 893 cm^{-1} is lower than the ν C-C stretch of CH$_3$CO$_2^-$(aq) located at 928 cm^{-1}. The ν C-C stretching mode for CH$_3$CO$_2^-$(aq) is a strong band in the acetate solution spectra and with its relatively small half width, it is well suited for speciation studies such as ion pair formation. The NaCH$_3$CO$_2$(aq) spectra revealed no signs of CIP formation between Na$^+$(aq) and CH$_3$CO$_2^-$(aq) but instead ion pairs with one water molecule interposed between Na$^+$ and CH$_3$CO$_2^-$ were invoked. The solvent separated ion pair of the form [Na(OH$_2$) CH$_3$CO$_2$]^0 exists in very concentrated sodium acetate solutions. It could be shown that in LiCH$_3$CO$_2$ solutions acetato-complexes occur in concentrated solutions and in the hydrate melt.

Intramolecular coupling of the modes in CH$_3$CO$_2^-$ and CH$_3$COOH is fairly extensive and therefore DFT calculations were carried out in order to compare the measured spectra with the calculated ones. The geometrical parameters such as bond length and bond angles of the acetate, and acetic acid were given and may be compared with those published for other acetates and carboxylic acids. Acetic acid, CH$_3$COOH(aq), is a weak acid and the pK$_a$ value derived from quantitative Raman measurements is equal to ~ 4.5 at 23 °C.

Literature

[1] B. Hess, and N. F. A. van der Vegt, *Proc. Natl. Acad. Sci. USA*, 2009, **106**, 13296-13300.

[2] J. S. Uejio, C. P. Schwartz, A. M. Duffin, W. S. Drisdell, R. C. Cohen, and R. J. Saykally, *Proc. Natl. Acad. Sci. USA*, 2008, **105**, 6809-6812.

[3]   J.-J Max, C. Chapados, *J. Phys. Chem. A*, 2004, **108**, 3324-3337.

[4] E. Gojlo, M. Smiechowski, A. Panuszko, J Stangret, *J. Phys. Chem*. B, 2009, **113**, 8128–8136.

[5] J. Stangret, T. Gampe, J. Phys. Chem. A, 2002, **106**, 5393-5402.

[6] H. M. A. Rahman, G. Hefter and R. Buchner, *J. Phys. Chem. B*, 2012, **116**, 314–323.

[7] H. M. A. Rahman and R. Buchner, *J. Mol. Liquids*, 2012, **176**, 93-100.

[8] K. D. Collins, *Biophys. J.*, 1997, **72**, 65-76.

[9] K. J. Wilmshursts, *J. Chem. Phys.*, 1955, **23**, 2463.

[10] L. H. Jones, and E. McLare, *J. Chem. Phys.*, 1954, **22**, 1796 -1800.

[11] K. Ito, and H. J. Bernstein, *Can. J. Chem.*, 1956, **34**, 170 -178.

[12] E. Spinner, *J. Chem. Soc.*, 1964, 4217 - 4226.

[13] M. Kakihana, M. Kotaka and M. Okamoto, *J. Phys. Chem.*, 1983, **87**, 2526-2535

[14] F. Quiles and A. Burneau, *Vib. Spectrosc.*, 1998, **16**, 105-117.

[15] M. M. Yang, D. A. Crerar and D. E. Irish, *Geochim. Cosmochim. Acta*, 1989, **53**, 319-326.

[16] R. I. Bickley, H. G. M. Edwards, S. J. Rose and R. Gustar, *J. Mol. Struct.*,1990, **238**, 15-26.

[17] Z. Nickolov, I. Ivanov, G. Georgiev and D. Stoilova, *J. Mol. Struct.*, 1996, **377**, 13-17.

[18] A. Wahab, S. Mahiuddin, G. Hefter, W. Kunz, B. Minofar, and P. Jungwirth, *J. Phys. Chem. B*, 2005, **109**, 24108-24120.

[19] I. A. Heisler and S. R. Meech, *Science*, 2010, **327**, 857-860.

[20] Y. Kameda, K. Sugawara, T. Usuki, and O. Uemura, *Bull. Chem. Soc. Jpn.,*1998, **71**, 2769-2776.

[21] S. Varma and S. B. Rempe, *Biophysical Chemistry*, 2006, **124**, 192–199.

[22] R. Mancinelli, A. Botti, F. Bruni, M. A. Ricci, A. K. Soper, *J. Phys. Chem. B*, 2007**, 111***, 13570-13577.

[23] S. S. Azam, T. S. Hofer, B. R. Randolf and B. M. Rode, *J. Phys. Chem. A*, 2009, **113**, 1827-1834.

[24] A. Bankura, V. Carnevale, M. L. Klein, *J. Chem. Phys.*, 2013,**138**, 014501-10.

[25] J. Mähler and I. Persson, *Inorg. Chem.*, 2012, **51**, 425−438.

[26] W. Rudolph and M. H. Brooker: Raman Studies of Lithium Coordination in Molten and Aqueous Environments., in Proceedings of the Ninth International Symposium on Molten Salts, Eds.: Ch.L. Hussey, D.S Newman, G. Mamantov and Y. Ito, Physical Electrochemistry Proceedings Vol. 94-13, The Electrochemical Society, Pennington, NJ, (1994), 235 - 241.

[27] Y. Kameda, H. Ebata, and O. Uemura, *Bull. Chem. Soc. Jpn.*, 1994, **67**, 929-935.

[28] W. W. Rudolph, M. H. Brooker and C. C. Pye, *J. Phys. Chem.*, 1995, **99**, 379-384

[29] W. W. Rudolph, G. Irmer, and G. T. Hefter, *Phys. Chem. Chem. Phys.*, 2003, **5**, 5253.

[30] W. W. Rudolph, and G. Irmer, *Dalton Trans*. 2013, **42**, 3919–3935.

[31] W. W. Rudolph, and G. Irmer, *Dalton Trans*. 2013, **42**, 14460-14472.

[32] W.W. Rudolph, and G. Irmer, *Appl. Spectrosc.*, 2007, **61**, 1312-1327.

[33] W. W. Rudolph, D. Fischer, G. Irmer, C. C. Pye, *Dalton Trans.,* 2009, 6513–6527.

[34] W. W. Rudolph and G. Irmer, *J. Sol. Chem.*, 1994, **23**, 663-674.

[35]Gaussian 03, Revision C.02, M. J. Frisch, G. W. Trucks, H. B. Schlegel, G. E. Scuseria, M. A. Robb, J. R. Cheeseman, J. A. Montgomery, Jr., T. Vreven, K. N. Kudin, J. C. Burant, J. M. Millam, S. S. Iyengar, J. Tomasi, V. Barone, B. Mennucci, M. Cossi, G. Scalmani, N. Rega, G. A. Petersson, H. Nakatsuji, M. Hada, M. Ehara, K. Toyota, R. Fukuda, J. Hasegawa, M. Ishida, T. Nakajima, Y. Honda, O. Kitao, H. Nakai, M. Klene, X. Li, J. E. Knox, H. P. Hratchian, J. B. Cross, V. Bakken, C. Adamo, J. Jaramillo, R. Gomperts, R. E. Stratmann, O. Yazyev, A. J. Austin, R. Cammi, C. Pomelli, J. W. Ochterski, P. Y. Ayala, K. Morokuma, G. A. Voth, P. Salvador, J. J. Dannenberg, V. G. Zakrzewski, S. Dapprich, A. D. Daniels, M. C. Strain, O.

16

Farkas, D. K. Malick, A. D. Rabuck, K. Raghavachari, J. B. Foresman, J. V. Ortiz, Q. Cui, A. G. Baboul, S. Clifford, J. Cioslowski, B. B. Stefanov, G. Liu, A. Liashenko, P. Piskorz, I. Komaromi, R. L. Martin, D. J. Fox, T. Keith, M. A. Al-Laham, C. Y. Peng, A. Nanayakkara, M. Challacombe, P. M. W. Gill, B. Johnson, W. Chen, M. W. Wong, C. Gonzalez, and J. A. Pople, Gaussian, Inc., Wallingford CT, 2004.

[36] M. Cossi, G. Scalmani, N. Rega, and V. Barone, *J. Chem. Phys.*, 2002, **117**, 43 – 54.

[37] C. Cappelli, S. Corni, R. Cammi, B. Mennucci and J. Tomasi, *J. Chem. Phys.*, 2000, **113**, 11270 – 11279.

[38] C. Cappelli, S. Corni, and J. Tomasi, *J. Chem. Phys.*, 2001, **115**, 5531 – 5535.

[39] D. T. Richens: The Chemistry of Aqua Ions. Chapter 2: Main Group Elements. Wiley & Sons, 1997.

[40] K. Leung, S. B. Rempe, and O. A. von Lilienfeld, *J. Chem. Phys.*, 2009, **130**, 204507-11.

[41] G. D. Markham, M. Trachtman, C. L. Bock and C. W. Bock*, J. Mol. Struct. (Theochem)*, 1998, **455**, 239 – 256.

[42] A. Payaka, A. Tongraar, B. M. Rode, *J. Phys. Chem. A*, 2010, **114**, 10443-10453.

[43] R. Caminiti, P. Cucca, M. Monduzzi, G. Saba, G. Crisponi, *J. Chem. Phys*. 1984, **81**, 543-551.

[44] Y. Kameda, M. Sasaki, M. Yaegashi, K. Tsuji, S. Oomori, S. Hino and T. Usuki, *J. Sol. Chem.,* 2004, **33**, 733-745.

[45] S. Kubota, M. Iwaizumi, Y. Ikegami and K. Shimokoshi, *J. Chem. Phys*.,1979, **71**, 4771-4776.

[46] B. Nicolaï, A. Cousson, F. Fillaux, *Chemical Physics*, 2003, **290**, 101-120.

[47] J. Kapita´n, L. Hecht and P. Bouř, *Phys. Chem. Chem. Phys*., 2008, **10**, 1003-1008.

[48] A. J. Wells, and E. B. Wilson, *J. Chem. Phys*., 1941, **9**, 314-318.

[49] R. L. Frost and J. T. Kloprogge, *J. Mol. Struct.*, 2000, **526**, 131-141.

[50] D. C. McKean, *Spectrochim. Acta*, *A*, 1973, **29**, 1559 -1674.

[51] S. K. Freeman, Applications of Laser Raman Spectroscopy, John Wiley & Sons, New York, 1974.

[52] G. Köbrich, in: H. Volkmann, (Ed.) Handbuch der Infrarot Spektroskopie, Verlag Chemie, Weinheim Bergstraße, 1972, pp. 329-376.

[53] W. W. Rudolph and G. Irmer, *Spectrochim. Acta A*, 2011, **79**, 1483 – 1492.

[54] M. L. Senent, *J. Math. Chem.*, 2011, **49**, 1424 – 1435.

[55] A. Apelblat, *J. Mol. Liquids*, 2002, **95**, 99 – 145.

17

Table 1. Geometrical parameters for the acetate of structure **I** (dihedral angle = 0°): bond lengths a_{ij} (in Å), angles α_{ijk} and dihedral angle d_{4215} of the $CH_3CO_2^-$ anion (see Fig. 2) derived from DFT calculations.

parameter	molecule *in vacuo*	molecule (with solvation sphere)
a12	1.561	1.533
a23	1.253	1.261
a24	1.252_5	1.259
a15	1.091	1.088
a16	1.093	1.091
a17	1.093	1.091
α324	128.84°	125.40°
α516	109.51°	109.30°
α517	109.51°	109.30°
α617	107.03°	107.04°
d4215	0°	0°

18

Table 2. Assignments of the normal modes of $CH_3CO_2^-(aq)$ measured in dilute $NaCH_3CO_2(aq)$.

Raman				infrared			B3LYP 6-311++ (3df,2pd)	B3LYP 6-311++ (3df,2pd) + solvation	numbering of modes and symmetry	assignment
v_{max} /cm^{-1}	fwhh / cm^{-1}	intensity	depol. ratio	v_{max} / cm^{-1}	fwhh / cm^{-1}	Integr. Intensity				
n.d.	-	-	-	n.d.	-	-	13.5	22.9	v_{15} (a″)	τCO_2
474	21	0.254	0.70	475	20	0.139	434.8	447.1	v_{10} (a′)	ρCO_2
620.7	21.3	0.262	0.75	621	16	0.538	616.7	624.3	v_{14} (a″)	ρCO_2
654.2	25.9	2.375	0.346	654	23.5	4.121	618.1	632.7	v_9 (a′)	δCO_2
928.4	11.4	9.874	0.054	928.3	10.5	0.959	864.4	900.8	v_8 (a′)	$v C\text{-}C$
1021.5	26.5	0.231	0.70	1021.3	15	2.242	996.8	1020.8	v_7 (a′)	ρCH_3
1052	27	0.032	0.75	1053	14	0.611	1034.1	1058.1	v_{13} (a″)	ρCH_3
1347.6	11	1.884	0.367	1347	12	1.115	1322.4	1359.9	v_6 (a′)	δCH_3
1413.5 *	24.6	15.07	0.26	1413.5	26.5	29.365	1350.8	1397.4	v_5 (a′)	$v_s CO_2$
1426 *	26	0.297	0.5	1428	24	9.481	1463.0	1460.6	v_{12} (a″)	δCH_2
1440 *	18	0.297	0.75	1440	18	1.701	1476.4	1477.2	v_4 (a′)	δCH_2
1556	44	1.238	0.62	1556	41	100.0	1650.4	1557.4	v_3 (a′)	$v_{as} CO_2$
2935.5	23.4	100.0	0.005	~2935 #	n.d.	n.d.	2998.4	3028.0	v_2 (a′)	$v_s CH_3$
2984	23.5	3.666	0.75	~2985 #	n.d.	n.d.	3056.7	3087.5	v_{11} (a″)	$v_{as} CH_3$
3014	34.6	4.832	0.7	n.d.	n.d.	n.d.	3075.3	3115.8	v_1 (a′)	$v_{as} CH_3$

  n.d. not detected

* bands severely overlapped

these modes are severely overlapped by the OH band of water

19

Table 3. Summary of overtones and combination bands in Raman spectra of $CH_3CO_2^-$(aq) .

peak position /cm^{-1}	ρ	fwhh /cm^{-1}	intensity	assignment
1125	0.75	30	0.042	$\nu_9+\nu_{10}=1128.2$
1239	0.55	22	0.053	$2*\nu_{14}=1241.4$
1672	0.2	27	0.304	$\nu_7+\nu_9=1675.7$
1854	0.1	21	0.119	$2*\nu_8=1856.8$
1580	0.3	28	0.107	$\nu_8+\nu_9=1582.6$
2040	0.32	21	0.035	$2*\nu_7=2043$
2100	0.08	22	0.101	$2*\nu_{13}=2104$
2272	0.15	15	0.019	$\nu_6+\nu_8=2276$
2336	0.03	30	0.220	$\nu_5+\nu_8=2341.6$
2395	0.75	18	0.007	$\nu_6+\nu_{13}=2399.6$
2458	0.75	27	0.102	$\nu_5+\nu_{13}=2465.2$
2482 (sh)	0.75	28	0.024	$\nu_4+\nu_{13}=2492$
2683	0.07	20	1.671	$2*\nu_6=2695.2$
2754	0.15	33	1.549	$\nu_5+\nu_6=2760.8$
2848	0.16	25	3.575	$2*\nu_{12}=2852$

20

Table 4. Raman data of the monomeric, hydrated acetic acid, $CH_3COOH(aq)$ in dilute aqueous solution.

Raman aqueous solution				Infrared	B3LYP isolated molecule	B3LYP + solvation	symmetry	Assignment
ν_{max} /cm^{-1}	intensity	fwhh/ cm^{-1}	ρ					
n.d.	-	-	-	n.d.	57.6	44.5	ν_{18} (a'')	τCH_3
460.5	2.27	26	dp	n.d.	425.0	436.8	ν_{12} (a')	$\delta_{ip}C\text{-}C\text{-}O$
n.d.	-	-	-	n.d.	544.6	532.5	ν_{17} (a'')	$\delta_{op}C\text{-}C\text{-}O + \tau OH$
600	0.83	17	dp	n.d.	585.7	591.1	ν_{11} (a')	$\delta O\text{-}C\text{-}O$
627.5	5.56	28	0.72	n.d.	664.0	635.4	ν_{16} (a'')	$\tau\ OH$
893	55.5	18.0	0.034	890	858.7	870.2	ν_{10} (a')	$\nu\ C\text{-}C$
1017	1.87	18	0.33	1016	999.4	1006.6	ν_9 (a')	$\gamma_s CH_3$
1052	0.08	20	0.75	1054	1069.8	1066.1	ν_{15} (a'')	$\gamma_a CH_3$
1296	3.28	39	0.48	1285	1202.0	1186.2	ν_8 (a')	$\delta C\text{-}O\text{-}H$
1364	1.51	18	0.38	1368	1336.1	1329.4	ν_7 (a')	$\nu C\text{-}O + \delta COH + \delta CH_3$
1378	1.86	24	0.064	1382	1409.5	1403.9	ν_6 (a')	δCH_3
1417	4.37	33	0.04	1416	1473.8	1462.7	ν_5 (a')	$\delta_s HCH_2$
1438	3.36	29	0.75	1437, sh	1479.3	1469.2	ν_{14} (a'')	$\delta_{as} HCH_2$
1712.5	54.02	44.0	0.11	1712	1819.6	1746.7	ν_4 (a')	$\nu C=O$
2944	100.00	14	0.017	2951	3052.2	3043.0	ν_3 (a')	νCH_3
2996	5.30	22	0.75	n.d.	3109.8	3101.9	ν_{13} (a'')	$\nu_{as} HCH_2$
3029	5.25	22	0.72	3030	3162.5	3153.9	ν_2 (a')	$\nu_s HCH_2$
3220	0.5	v.br.	0.1	3247	3762.3	3268.8	ν_1 (a')	νOH

n.d.: not detected; sh: shoulder; v.br.: very broad
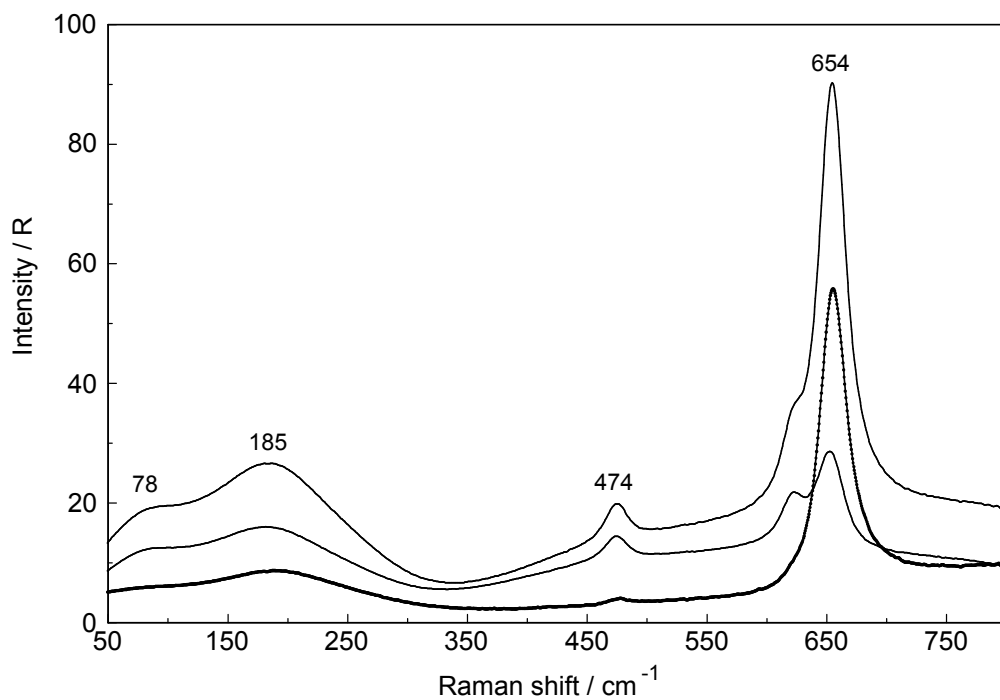
Figure 1 A. Raman spectrum (polarized, depolarized and isotropic) of a 2.183 molL^{-1} (R$_w$ = 22.90) NaCH$_3$CO$_2$ solution from 50-800 cm^{-1}.
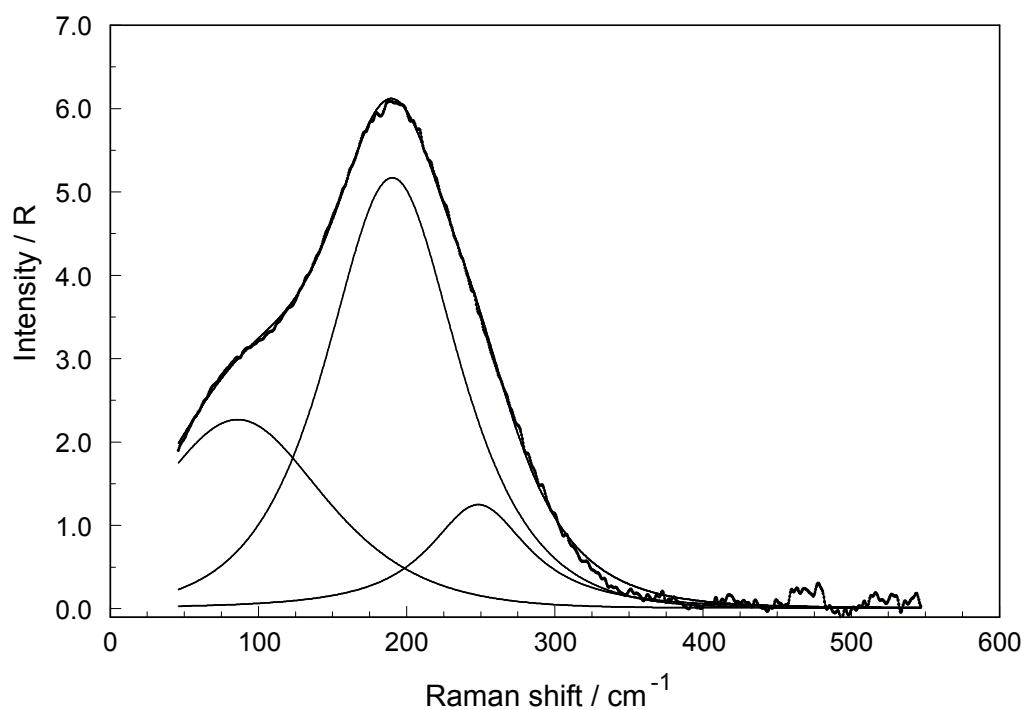

Figure 1 B. Isotropic Raman spectrum, sum curve and band components of the fit of a 2.183 mol·L^{-1} (R$_w$ = 22.90) NaCH$_3$CO$_2$ solution from 43-550 cm^{-1}. The component bands appear at: 80 cm^{-1}, 189 cm^{-1} and 245 cm^{-1}.

22
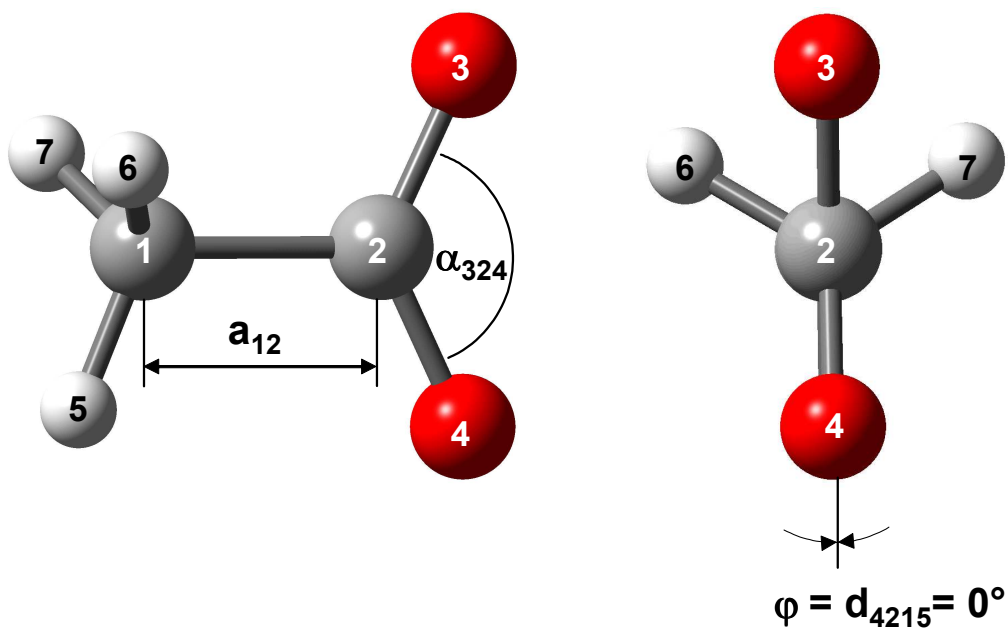
Figure 2. Gas phase geometry of $CH_3CO_2^-$ for $\varphi = 0°$. Left Figure: numbering of the atoms and definition of C-C bond distance and $-CO_2^-$ angle; Right Figure: projection viewed down the axis of the carbon atoms.

23
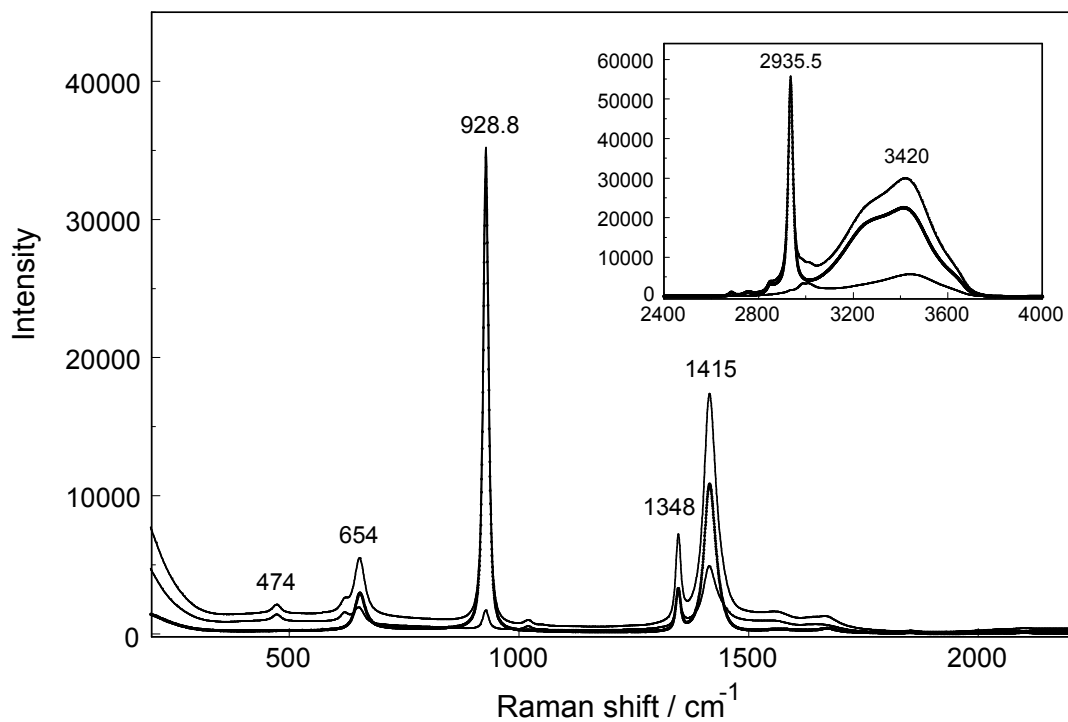
Figure 3 A. Overview Raman spectrum of an aqueous solution, 5.022 mol·L^{-1} (R$_w$ = 8.54), of NaCH$_3$CO$_2$ The inset contains the high frequency range from 2400 - 4000 cm^{-1} showing the ν C-H modes of CH$_3$CO$_2^-$(aq) and the very broad OH stretching band of water. Note, that all three scattering orientations are given: polarized, depolarized and isotropic.
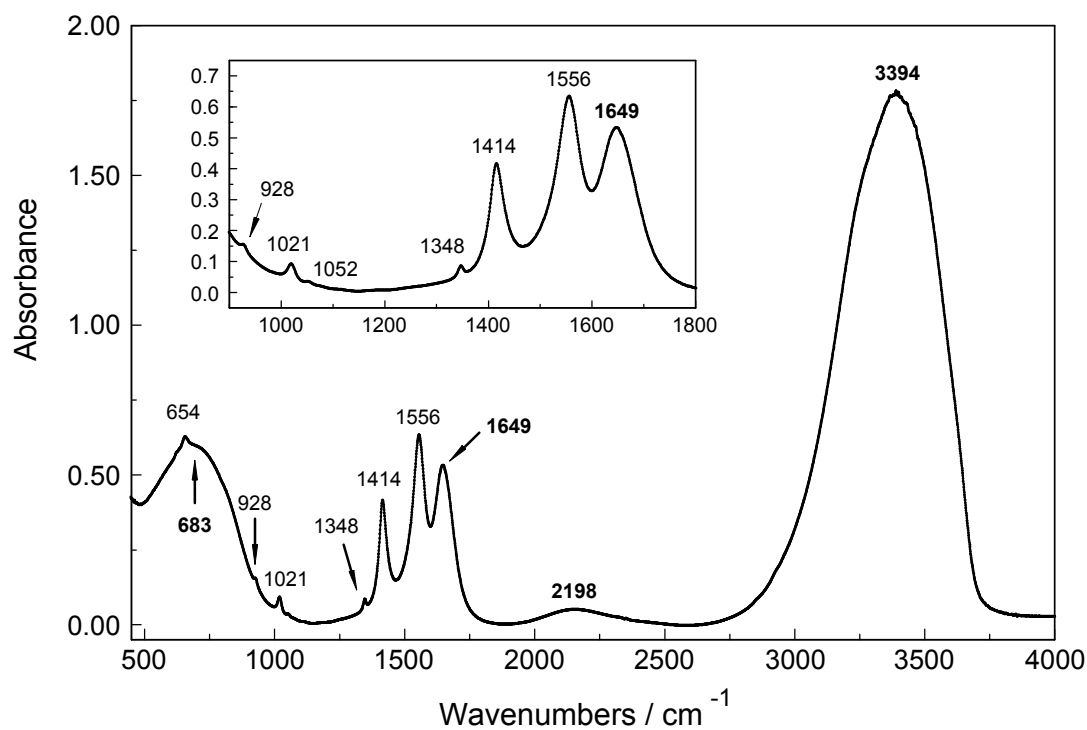
Figure 3 B. Overview infrared spectrum of an aqueous solution of $NaCH_3CO_2$ (2.183 mol·L^{-1} (R_w = 22.90)). The inset contains the mid infrared frequency range from 900 - 1800 cm^{-1} at an enlarged scale. The frequency values in bold face are assigned to water modes: the very broad band at 683 cm^{-1} is assigned to the rocking mode of H_2O, the mode at 1649 cm^{-1} is due to the deformation mode, the absorption at 2198 cm^{-1} is a combination band and the very broad and strong feature peaking at 3394 cm^{-1} is assigned to the O-H stretching.
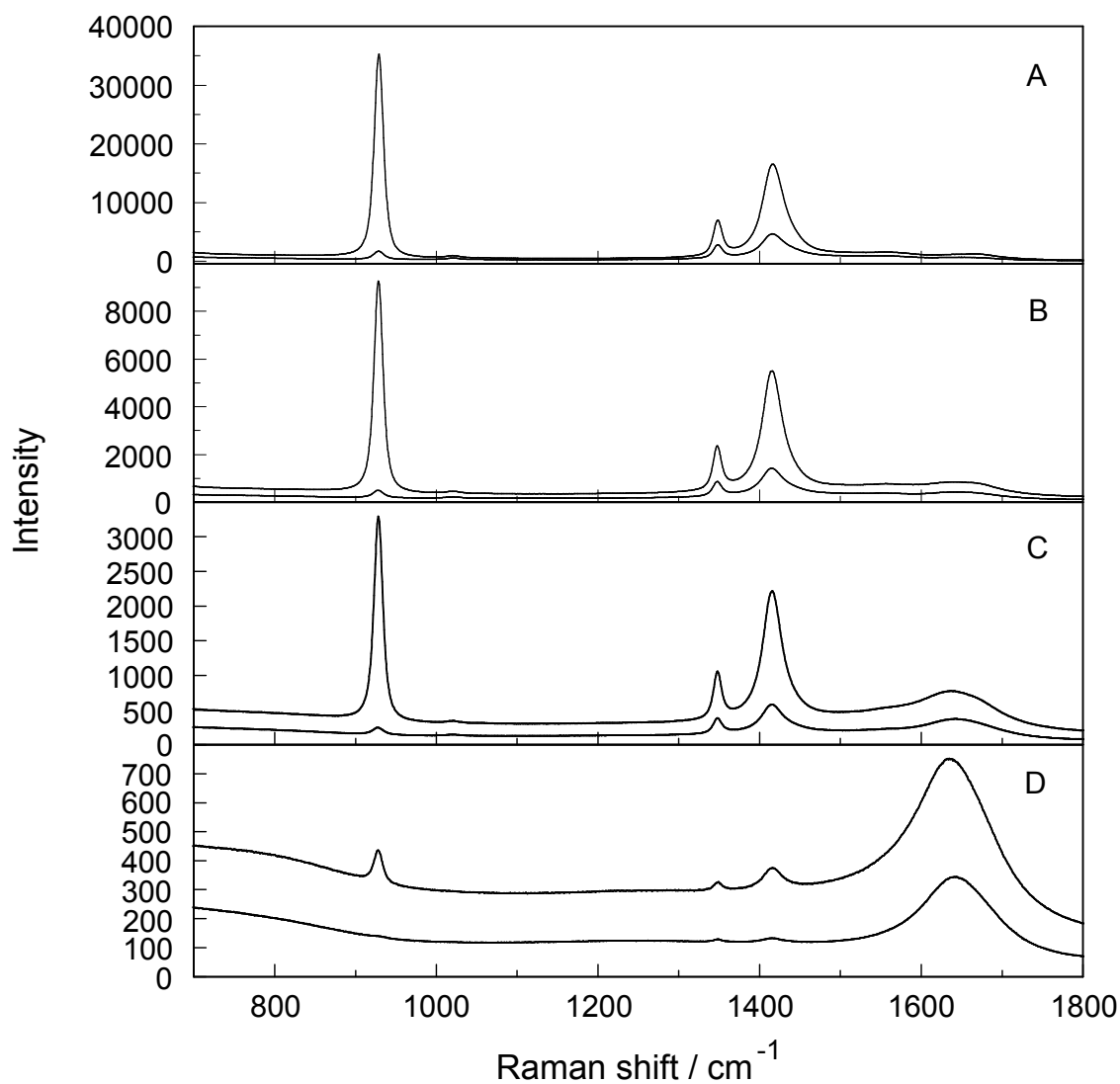
Figure 4. Raman spectra (I-polarized and I-depolarized) of A: 5.022 molL^{-1} (R$_w$ = 8.54); B: 2.183 molL^{-1} (R$_w$ = 22.90); C: 0.810 molL^{-1} (R$_w$ = 65.97) and D: 0.0325 molL^{-1}(R$_w$ = 1705) aqueous NaCH$_3$CO$_2$ solutions. Note, that the broad mode at 1642 cm^{-1} is due to the water deformation band. With increasing dilution its intensity is growing and finally dominates the spectrum.
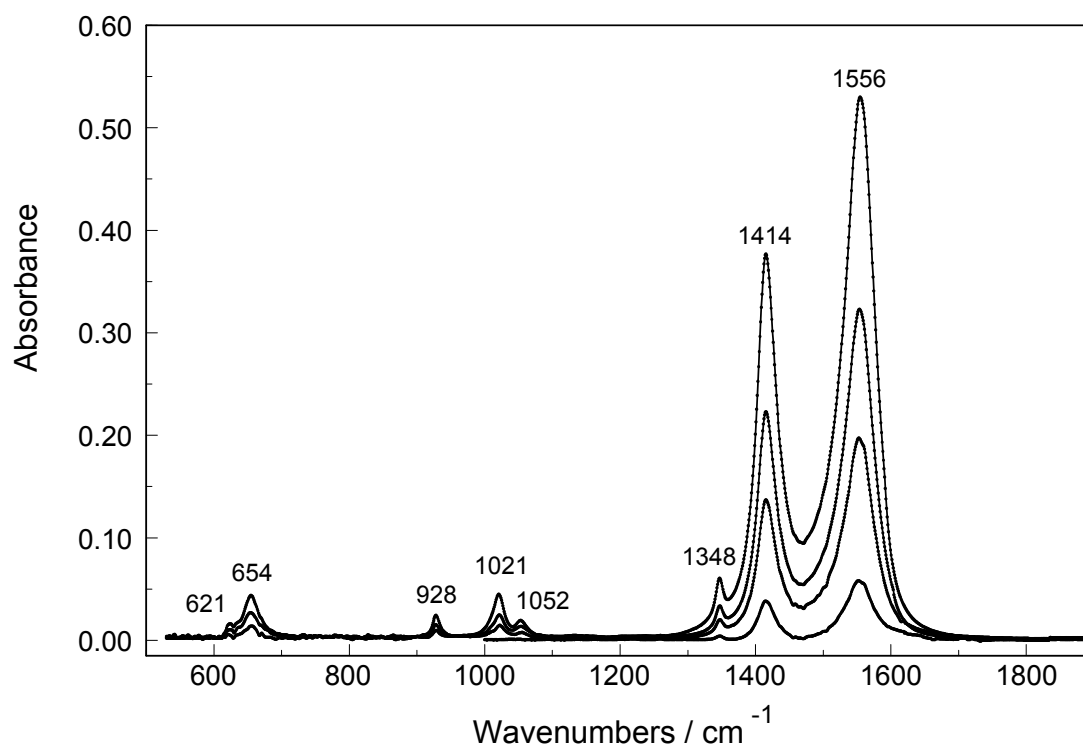
Figure 5. Infrared spectra, water spectra subtracted and baseline corrected, of aqueous $NaCH_3CO_2$ solutions. From top to bottom: A: 2.183 mol·L^{-1} (R_w = 22.90); B: 1.209 mol·L^{-1} (R_w = 43.40); C: 0.810 mol·L^{-1} (R_w = 65.97) and D: 0.161 mol·L^{-1} (R_w = 343.2).

27
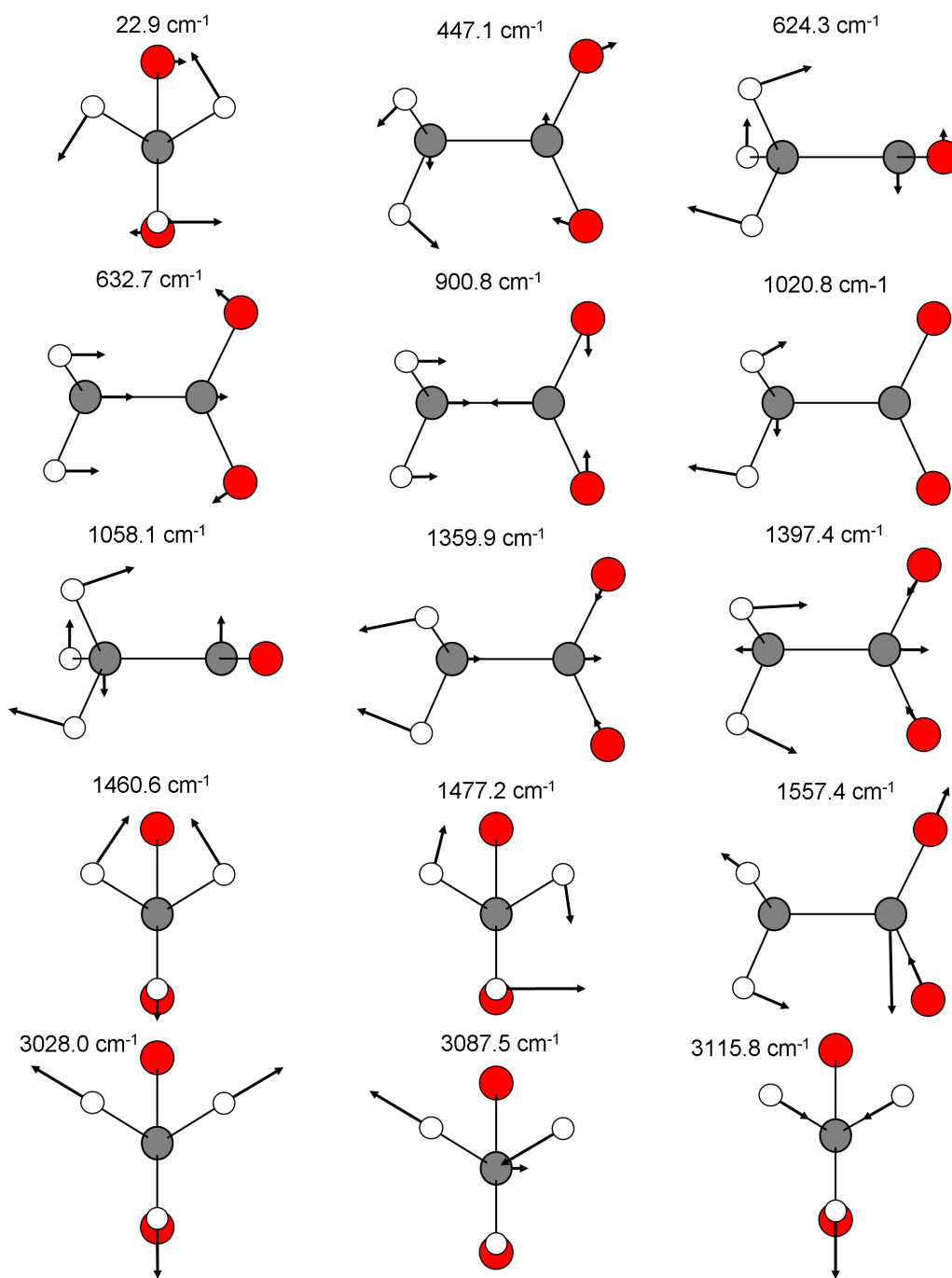
Figure 6. Normal vibrations of the $CH_3CO_2^-$ ion in solution, dihedral angle $\varphi = 0°$. Shown are the largest displacements of the atoms. The small open circles denote the H-atoms; the dark circles both C-atoms and the two red circles the oxygen atoms.
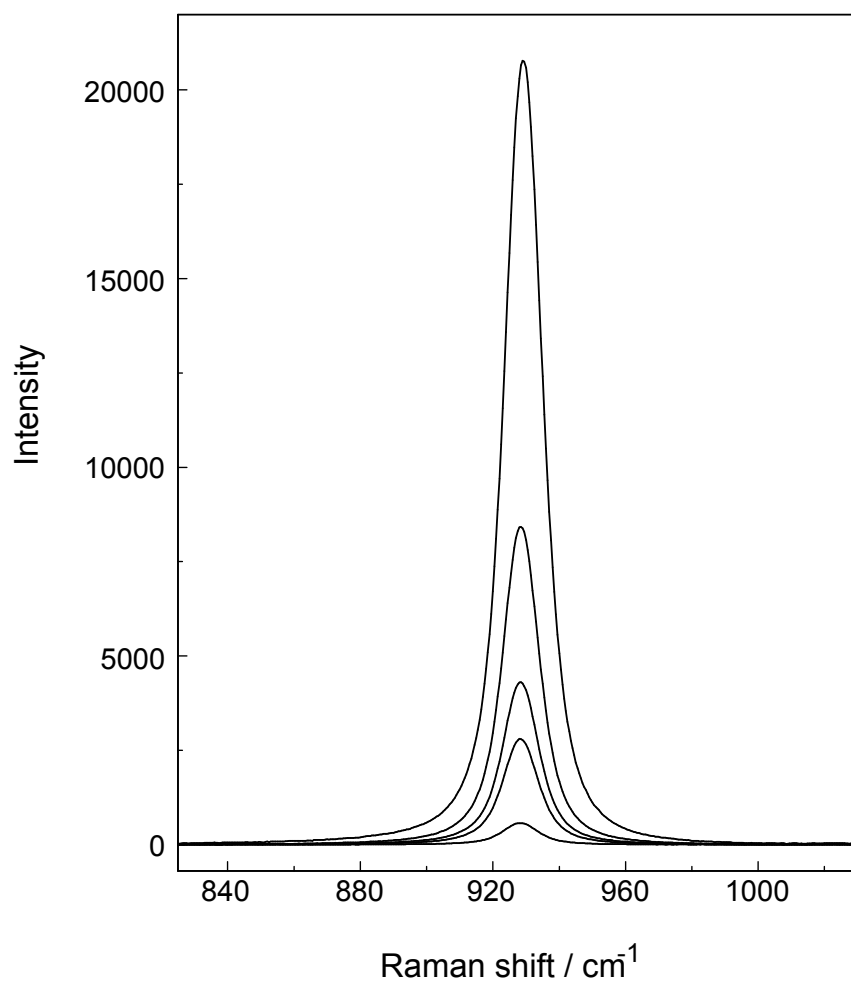
Figure 7 A. Isotropic Raman profiles, baseline corrected, of the ν C-C stretching mode of $CH_3CO_2^-$ (aq) as a function of the concentration of sodium acetate. From bottom to top: 0.161, 0.810, 1.209, 2.184, and 5.022 mol·L^{-1}.
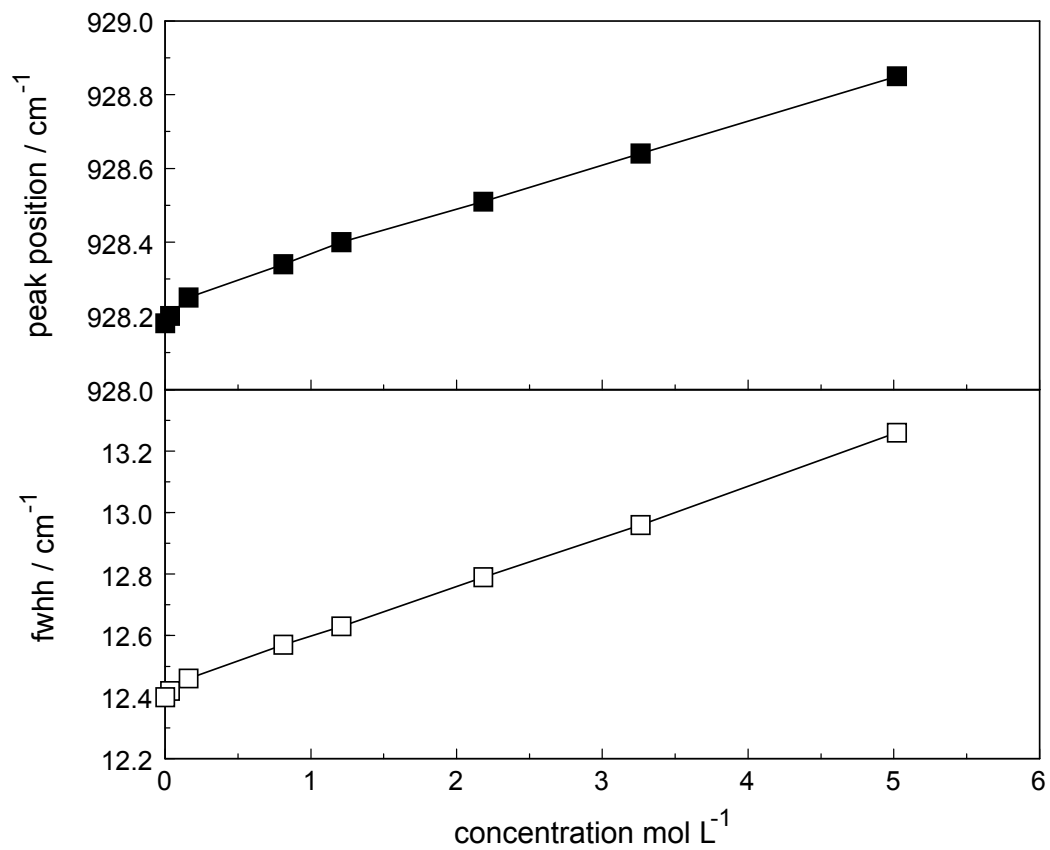
Figure 7 B. Peak position and fwhh (both in cm^{-1}) of the ν C-C stretching mode of CH$_3$CO$_2^-$(aq) as a function of the concentration of sodium acetate. Upper panel: filled squares, peak position; Lower panel: open squares, fwhh.
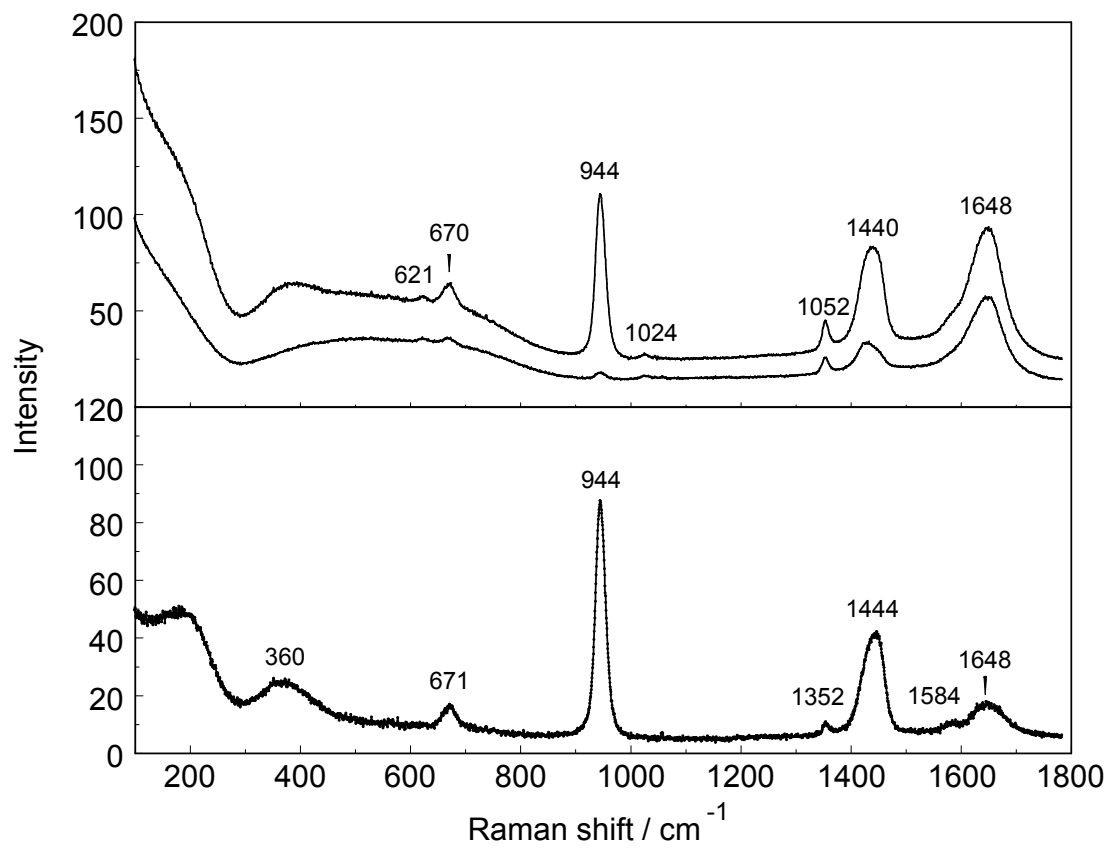
30

Figure 8. A 0.93 molL^{-1} LiCH$_3$CO$_2$ solution with an excess of LiCl added (13.56 molL^{-1}). Upper panel: I$_{VV}$ and I$_{VH}$; Lower panel: I$_{iso}$.

31

$$\varphi = d_{4215} = 0°$$

$$d_{4238} = 0°$$
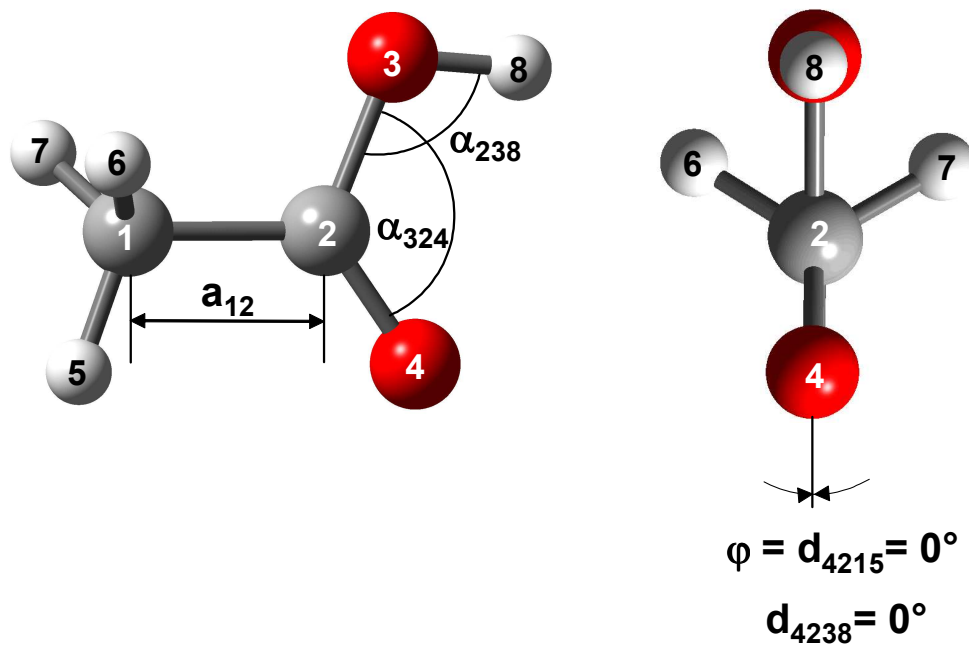
Figure 9. Geometry of the *trans* conformer of CH_3COOH conformational isomer with $\varphi = 0°$ in the gas phase.

32
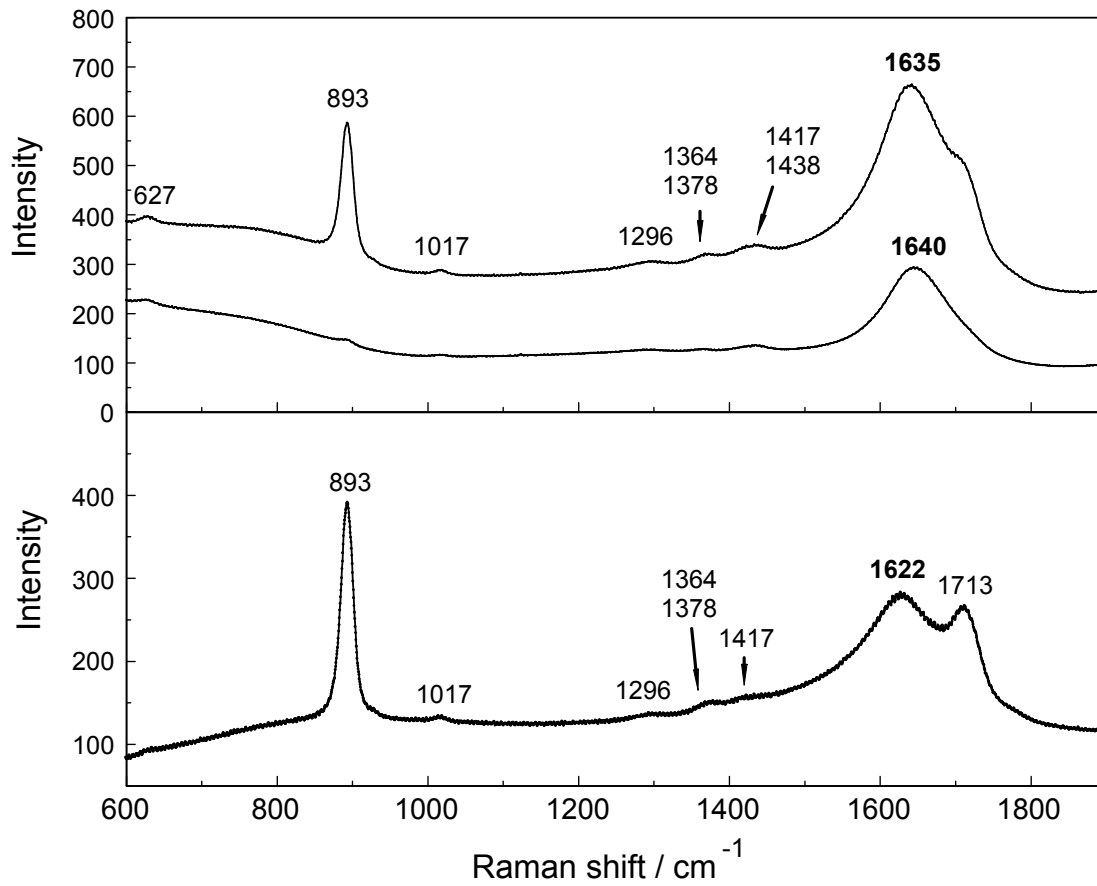
Figure 10. Raman scattering profiles, I_{VV} and I_{VH} at upper panel and I_{iso} at lower panel, of a 0.121 mol·L^{-1} CH$_3$COOH solution (R$_w$ = 453.8) at 23 °C. Note, that the wavenumber values for the water deformation mode are given in bold face. The deformation band shows the so called Raman non-coincidence effect.
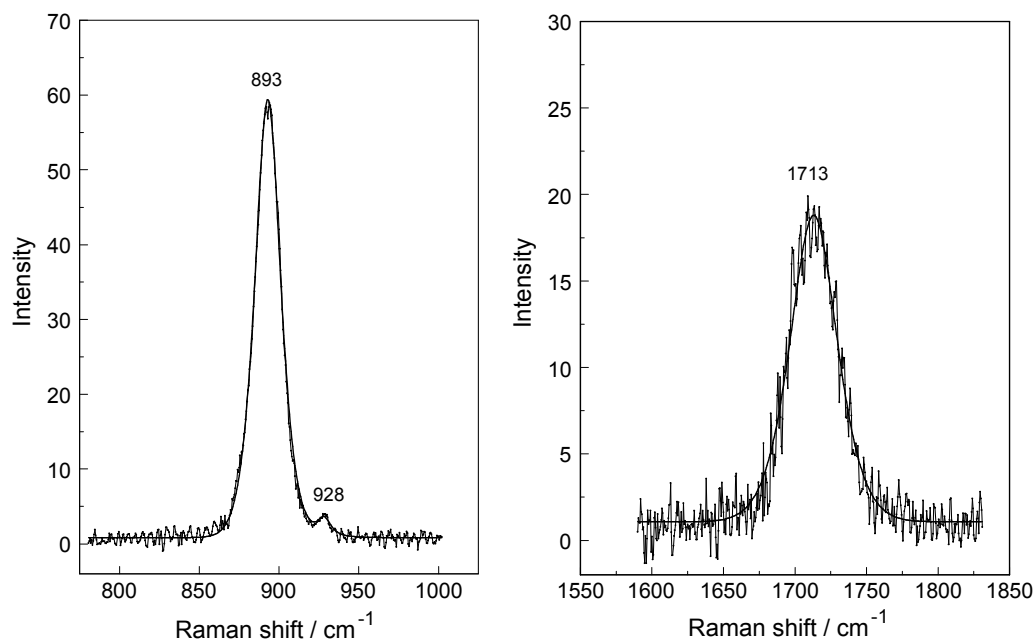
33

Figure 11. Left panel: The isotropic Raman profile, isotropic Raman spectrum of water subtracted, of a dilute aqueous CH_3COOH solution at 0.0246 mol·L^{-1} (R_w = 2241.4). Note, the ν C-C of CH_3COOH(aq) at 893 cm^{-1} (fwhh = 19 cm^{-1}) and at higher frequencies at 928.4 cm^{-1} the very small band from ν C-C of $CH_3CO_2^-$(aq). Right panel: The isotropic Raman profile, difference spectrum, of ν C=O of the same aqueous CH_3COOH solution. The ν C=O mode appears at (1712.8 ± 1) cm^{-1} (fwhh = (39.5 ± 2) cm^{-1}).

34

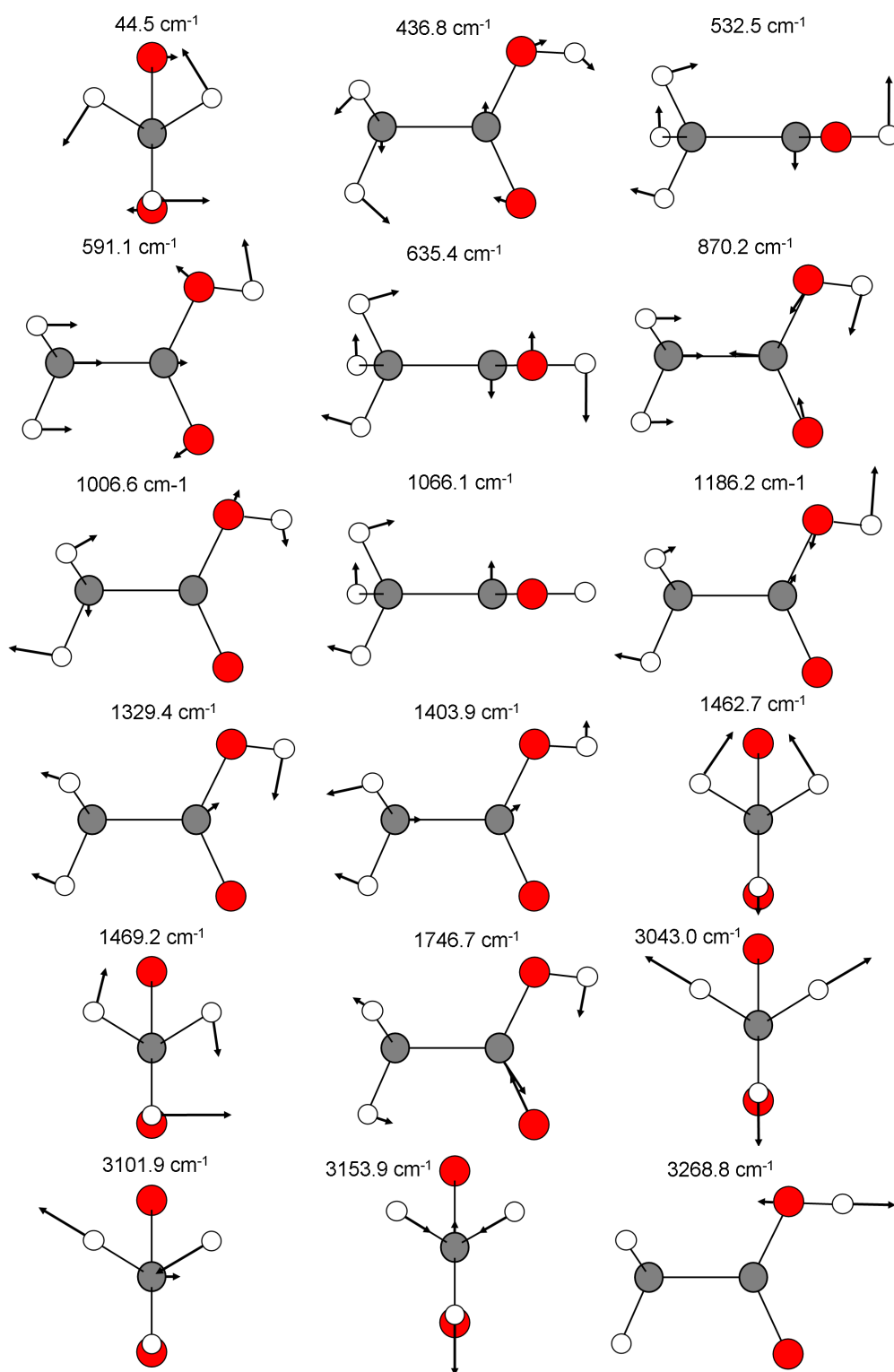**Figure 12.** Normal vibrations of CH₃COOH in aqueous solution, and dihedral angle φ = 0°. Shown are the largest displacements of the atoms. The small open circles denote the H-atoms; the dark circles both C-atoms and the two red circles the oxygen atoms.